Available online at www.sciencedirect.com
ScienceDirect
International Journal of Mass Spectrometry 255–256 (2006) 130–138
International Journal of Mass Spectrometry
www.elsevier.com/locate/ijms

Dissociation reactions of protonated anthracycline antibiotics following electrospray ionization-tandem mass spectrometry

Lekha Sleno[a,b], Valérie Campagna-Slater[a], Dietrich A. Volmer[a,b,*]

[a] *Department of Chemistry, Dalhousie University, Halifax, NS, Canada B3H 4J3*
[b] *Institute for Marine Biosciences, National Research Council, 1411 Oxford St., Halifax, NS, Canada B3H 3Z1*

Received 2 November 2005; received in revised form 6 February 2006; accepted 6 February 2006
Available online 7 March 2006

Abstract

Fragmentation pathways of doxorubicin, a common cancer therapy agent, and three closely related analogs (epirubicin, daunorubicin, idarubicin) were compared using electrospray ionization with tandem mass spectrometry. This class of antibiotics with anti-tumour activity has important structural features, with a tetracyclic aromatic, polyketide portion, which is glycosylated with an amino sugar in order to exhibit its biological activity. Collision-induced dissociation spectra revealed very similar product ions for each analog, however, important differences were seen in the relative abundances and the ease at which certain fragments were formed. Fragment ions observed included those from cleavage of the glycosidic bond, loss of the side chain from the aglycone moiety, water losses and loss of a methyl radical. Following cleavage of the glycosidic bond, the charge can either reside on the aglycone portion or the sugar moiety, and each of these primary fragments undergoes several secondary dissociation pathways, depending on the collision energy. By ramping the collision voltage, we were able to correlate the changes in fragmentation behavior with small alterations in the structure of the precursor ion. The detailed study of the fragmentation behavior of doxorubicin was supported by accurate mass measurements, using an electrospray-time of flight instrument, as well as MS^3 data from a quadrupole-linear ion trap mass spectrometer. Computational studies were also performed to help explain the role of certain functional groups in the fragmentation reactions.

Keywords: Anthracycline antibiotic; Doxorubicin; Fragmentation mechanism; Tandem mass spectrometry; Computational chemistry

1. Introduction

Doxorubicin, a commonly prescribed treatment in several cancers [1,2], belongs to the family of anthracycline antibiotics. Anthracyclines have been researched as cancer therapies for over 30 years and several structural analogs have been discovered through natural sources (e.g., *Streptomyces* bacteria) or synthesized, yielding different modes of action, potencies, targets and side effects [3]. The structure of these drugs includes a planar tetracyclic quinoid aglycone (anthracycline) with an aminoglycoside sugar (daunosamine) attached through an *O*-glycosidic bond (Fig. 1). The therapeutic effect of this class of drugs is exhibited by stabilizing the complex between the topoisomerase IIα enzyme and DNA in the cell's nucleus [4]. Doxorubicin and daunorubicin have been used as antitumour antibiotics with potent activity against solid tumours and some leukemias. Several analogs have since been developed with the aim of improving the spectrum of activity or to lower toxicity, including epirubicin [5] and idarubicin [6].

There have been many reports on the analysis of doxorubicin and related drugs by mass spectrometry. This technique has allowed the accurate quantitation of these drugs in biological matrices [7–9], as well as the analysis of drug-DNA complexes [10–12] and has also aided in the identification of numerous metabolites formed both in vitro and in vivo [13–16]. There have been numerous studies on the fragmentation of anthracyclines, using electron ionization (EI) [13,14,17–19], chemical ionization (CI) [19–21], field desorption [22,23], fast atom bombardment (FAB) [24,25] and thermospray [19]. There has been no detailed investigation, however, using tandem mass spectrometry (MS/MS) with electrospray ionization (ESI). ESI has been applied to the analysis of anthracycline antibiotics previously, but mainly in quantitative applications. One previous report used in-source fragmentation for quantitation [7], while

* Corresponding author. Tel.: +1 902 426 4356; fax: +1 902 426 9259.
E-mail address: Dietrich.Volmer@nrc-cnrc.gc.ca (D.A. Volmer).

1387-3806/$ – see front matter © 2006 Elsevier B.V. All rights reserved.
doi:10.1016/j.ijms.2006.02.003

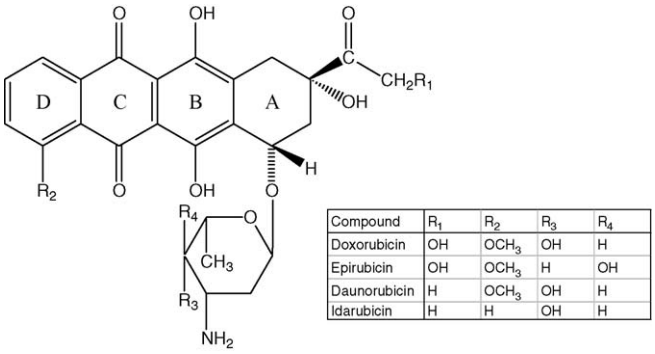

Compound	R_1	R_2	R_3	R_4
Doxorubicin	OH	OCH_3	OH	H
Epirubicin	OH	OCH_3	H	OH
Daunorubicin	H	OCH_3	OH	H
Idarubicin	H	H	OH	H

Fig. 1. Structures of doxorubicin and three structurally similar anthracycline drugs (daunorubicin, epirubicin, idarubicin).

others implemented the higher selectivity technique of multiple-reaction monitoring (MRM) for quantifying anthracyclines in urine [8] or doxorubicin and metabolites in rat plasma and tissue samples [9]. Some fragmentation studies have been reported for anthracyclines [19–21,23–25], including some by FAB and CI-MS. Anthracyclines reveal an array of dissociation pathways by which they can form characteristic product ions. ESI, on the other hand, is a very soft method of ionization, yielding mostly protonated molecules. In this case, subsequent activation by tandem mass spectrometry can aid in the structural elucidation of analogous compounds such as metabolites or degradation products, and could also be useful for a more fundamental understanding of ion structure and stabilizing effects causing certain pathways to be favored under specific conditions.

ESI-MS/MS has a further advantage for this compound class since it has also been proven to be very useful for the analysis of anthracyclinones (aglycones) in positive ion mode, and therefore any analogs or metabolites of doxorubicin (or a related drug) can also be analysed under similar conditions. In a previous study [24], the mass spectral characterization of several anthracyclines and corresponding aglycones was performed using fast atom bombardment. The aglycones were not ionizable in the positive ion mode, and therefore had to be characterized as negative ions. Also, no low mass fragments were monitored. Another problem with FAB spectra is that often there is a mix of molecular ions and protonated ions, causing the spectra to be potentially derived from fragments from several precursors. Understanding all the fragmentation pathways for the anthracycline parent compound could also help in the elucidation of metabolites, even if the glycosidic bond has been cleaved. Main metabolic pathways for doxorubicin include the reduction of the keto group at C-13, cleavage of the glycosidic bond and conjugation with a glucuronide moiety [14]. Importantly, all these metabolites can be ionized with electrospray in positive ion mode. If a new anthracycline drug would be assessed for metabolic pathways, ESI-MS/MS would be the method of choice for gaining important structural information, especially if there is a limited amount of sample.

This study describes the dissociative behavior of doxorubicin and three structurally similar compounds (epirubicin, daunorubicin, idarubicin). Epirubicin differs from doxorubicin only in the stereochemistry of a single hydroxyl group in the sugar moiety (4′epi daunosamine). Daunorubicin is structurally identical to doxorubicin, except the hydroxyl group at position C-14 on the A ring side chain is removed (Fig. 1). Idarubicin also has the same side chain as daunorubicin and has an additional structural difference in the D ring, caused by the removal of the methoxy group. Since all of these structures are extremely similar, we would also expect their mass spectrometric behavior to be quite comparable. Any differences we would observe in their fragmentation behavior should then be directly related to these small changes in the above-mentioned functional groups. In turn, more can be understood on their behavior when ionized in the gas-phase. Certain pathways are seen to occur more readily in some structurally similar analogs versus others. All major fragmentation reactions of these anthracyclines were studied in detail using tandem mass spectrometry, accurate mass data as well as some computational calculations to further rationalize some of the proposed pathways.

2. Experimental

2.1. Materials

Doxorubicin hydrochloride, epirubicin hydrochloride, daunorubicin hydrochloride idarubicin hydrochloride, and formic acid were purchased from Sigma (Mississauga, Ont., Canada). Methanol (Caledon, Georgetown, Ont., Canada) and Milli-Q organic-free water (Millipore, Bedford, MA, USA) were used as solvents.

2.2. Mass spectrometry

Collision-induced dissociation (CID) spectra were acquired in the positive ion mode on a MDS Sciex (Concord, Ont., Canada) API 4000 triple quadrupole mass spectrometer with direct infusion of each anthracycline at a concentration of 10 μM in 50% methanol, 0.05% formic acid at a flow rate of 25 μl/min. The instrument was operated with a spray voltage of 5.5 kV, a declustering potential of 50 V, a source temperature of 100 °C, a GS1 value of 50 and the curtain gas set at 10. Ultra-pure nitrogen was used as both curtain gas and collision gas. MS/MS spectra of the protonated molecule of each drug were acquired and MRM

Table 1
Corresponding fragment ion masses for doxorubicin and its three analogs

MH^+	$-H_2O$	Aglycone	CH_2OH (side chain)	–Side chain	$-CH_3$ radical	Sugar	Sugar fragments
Dox/Epi (544)	526/508	415/397/379	361/346/333	321	306	148/130	113/95/86/72/69
Dau (528)	510/484	399/381/363	n/a	291	n/a	148/130	113/95/86/72/69
Ida (498)	480/462	369/351/333	n/a	291	n/a	148/130	113/95/86/72/69

Table 2
MS^3 results for doxorubicin

m/z of precursor	CE (q_2)	Ions detected
544	5	**526**, **508**, **490**, **415**, 398, **397**, **379**, **361**, **346**, **333**, **321**
526	12	**508**, **490**, 472, 423, 414, **397**, **379**, **361**, 351, 337, **321**
508	20	491, **490**, 473, 472, **397**, 396, 380, **379**, **361**, **346**, 337, **321**
415	10	**397**, **379**, **361**, **321**
397	15	**379**, **361**, 351, **346**, **333**, **321**
379	25	**361**, 351, **346**, **333**, **321**
361	37	**346**, **333**
346	57	–
333	42	331, 318, 315, 305, 303, 287, 275, 259, 145
321	37	**306**, 293, 277, 262
306	65	–
148	20	**130**
130	23	**113**, **95**, **86**, **72**, **69**
113	35	**95**, 85, **69**
95	50	67
86	50	–

transitions for important fragments (see Table 1) were monitored as the collision energy was ramped from 5–100 V (step size 0.5 V). The data for the fragment ion curves represent an average of five consecutive experiments.

MS^3 data were acquired on a MDS Sciex 4000 QTRAP (quadrupole-linear ion trap) system with the doxorubicin stock solution directly infused into the ion source at a flow rate of 25 μl/min. Source parameters were as follows: spray voltage 5.5 kV, declustering potential 40 V, source temperature 100 °C, GS1 20 and curtain gas set at 10. Optimal CID conditions in q_2 (see Table 2) were chosen to have maximal ion abundances for each ion chosen for secondary activation in the linear ion trap (LIT). Conditions in the LIT were: dynamic fill on, excitation energy of 100 V and excitation time of 100 ms.

Accurate mass measurements were performed on an Agilent (Wilmington, DE, USA) LC/MSD TOF, equipped with an 1100 Agilent HPLC system, with a capillary voltage of 3 kV, source temperature at 350 °C and fragmentor voltage of 125 V for $(M+H)^+$ and 250 V for fragment ions. LC/MS was performed for these measurements with mobile phases: A; water, B; acetonitrile, both with 0.05% formic acid. Gradient elution was as follows: 0.5 min isocratic at 15% B, followed by linear increase to 50% to 15 min on a Zorbax SB-C18 rapid resolution, 1.8 μm, 30 mm × 2.1 mm column at 0.1 ml/min. Internal mass calibration with *m/z* 121.050873 and 922.009827 (present in the Agilent ESI Tuning mix) delivered by the second sprayer of the dual electrospray source. Some measurements were conducted with loop injections of a standard solution of doxorubicin.

2.3. Computational methods

Calculations were carried out using the Gaussian 03 program [26]. Density functional theory was used to perform all calculations, employing the B3LYP hybrid functional [27,28]. Geometries were optimized (6-31G* basis set), and vibrational analyses were conducted in order to verify optimized geometries. Single-point energy calculations (6-311+G** basis set) were then performed. The reported energies include the zero-point vibrational energies (ZPE), obtained from the B3LYP/6-31G* vibrational analyses and scaled by 0.9806 [29]. This method will be referred to as B3LYP/6-311+G**//B3LYP/6-31G* for simplicity.

The absolute proton affinity (APA) in the gas-phase is defined as the standard enthalpy of reaction:

$$BH^+ \rightarrow B + H^+ \quad (1)$$

This can be readily calculated from energy calculations and vibrational analyses:

$$APA = \Delta H = \Delta E_{elec} + \Delta E_{ZPE} + \Delta E_{int(298.15)} + (5/2)RT \quad (2)$$

The ΔE_{elec} term is the difference in electronic energy between the base (B) and its conjugate acid (BH^+), ΔE_{ZPE} the difference in zero-point vibrational energy, $\Delta E_{int(298.15)}$ the difference in thermal energy at 298.15 K, and (5/2)RT includes the PV term and the translational energy of the proton [30,31].

Geometries and electronic energies for the unprotonated and protonated structures were obtained with the B3LYP/6-311+G**//B3LYP/6-31G* method. Vibrational analyses were performed at the B3LYP/6-31G* level to determine the ZPE and thermal energy corrections [29]. Basis set superposition error (BSSE) corrections were estimated using the Boys-Bernardi counterpoise method [32]. For each molecule, the hydrogen atom was removed from its protonated B3LYP/6-31G* optimized geometry, and a B3LYP/6-311+G** single-point energy calculation was performed on this structure with and without ghost functions at the site of protonation. These corrections are included in all reported proton affinity values.

3. Results and discussion

An extensive study of the fragmentation reactions of four anthracycline drugs (doxorubicin, epirubicin, daunorubicin, idarubicin) has been performed using tandem mass spectrometry following electrospray ionization. Several differences in the behavior of their protonated molecules following ion activation were seen, since certain fragmentation channels are more easily accessed in some of these analogs, presumably due to differences in stabilities or proton affinities of the product ions. The fragmentation of doxorubicin was initially studied in detail with tandem mass spectrometry, including MS/MS and MS^3 data. Accurate mass measurements also assisted in the elucidation of the dissociation reactions with corresponding ion structures for the product ions of doxorubicin. This section consists of a preliminary discussion of the fragmentation of doxorubicin from CID experiments in a triple quadrupole, followed by the presentation of MS^3 and accurate mass data. A fragmentation scheme is then shown detailing the important dissociation pathways of this molecule with a comparison to the other anthracycline drugs. Computational data was used to support the proposed fragmentation pathways and characterize absolute proton affinities for some the discussed ions.

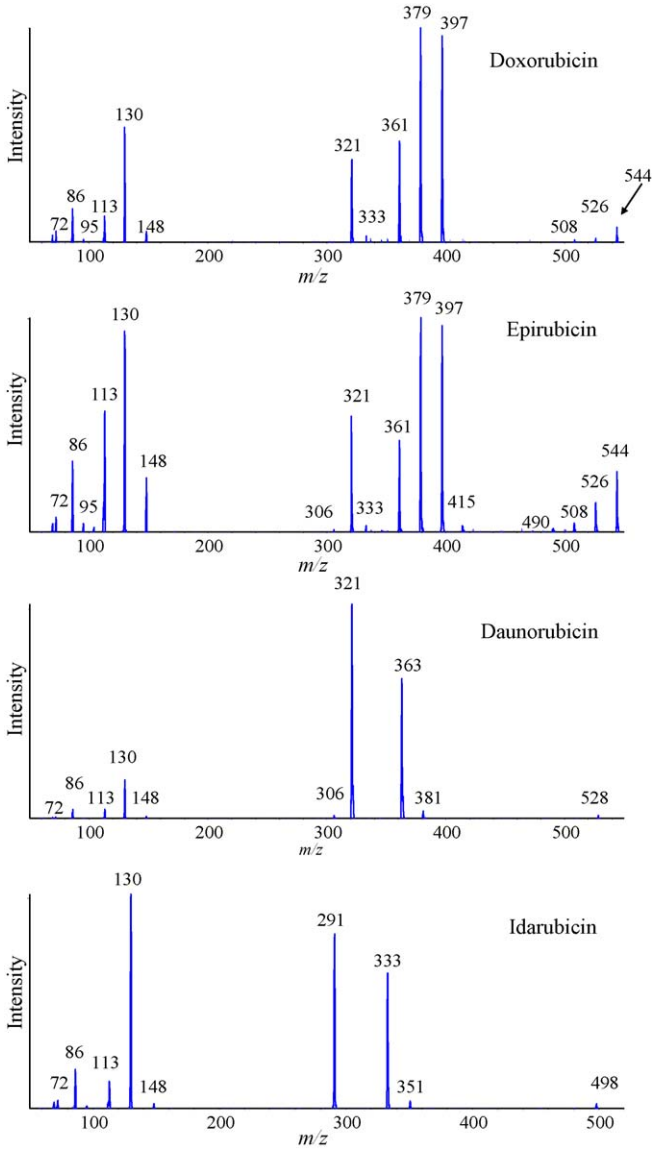

Fig. 2. CID spectra for the four investigated drugs at a collision offset voltage of 25 V.

3.1. Elucidating the detailed fragmentation mechanisms for doxorubicin

Doxorubicin and its analogs exhibit similar fragmentation reactions following collision-induced dissociation (CID). Table 1 lists the different fragment ions for doxorubicin and the corresponding *m/z* values for the analogous product ions of the other three molecules. The main pathways include the cleavage of the glycosidic bond with the charge either residing on the aglycone moiety or the sugar portion, cleavage of the side chain on the A ring, and further small neutral losses, such as H_2O, NH_3 and CO. The CID spectra for each of the four analogs are shown in Fig. 2. These spectra exhibit three main groupings of ions; one due to the protonated molecule with some water losses, a cluster of ions due to the aglycone portion with additional neutral losses and a third group in the low mass range for the ions of the daunosamine sugar. It is easily seen that several fragmentation pathways are lost for the aglycone portion due to the changes in the precursor ion structure, as in the case of daunorubicin and idarubicin. The side chain hydroxyl group, which is missing in both of these molecules, must be central in an important fragmentation reaction (vide infra). Epirubicin also shows a more important water loss fragment from the protonated molecule, potentially due to the different orientation of the hydroxyl group in the sugar group (4′epi daunosamine).

Additional information for the elucidation of complex fragmentation pathways can be gained by using multiple stages of tandem mass spectrometry (e.g., in a conventional 3D-ion trap [33] or in a quadrupole-linear ion trap (QqLIT) [34]). Using a second stage of MS/MS in the linear ion trap of a QqLIT instrument provided important information for the assignment of dissociation reactions. The conditions in the second quadrupole (collision cell, q_2) were individually optimized for the formation of each product ion of doxorubicin seen in the triple quadrupole spectra. Several experiments were subsequently conducted with on-resonance CID in the LIT, producing fragment ions derived only from the isolated product ion initially formed in q_2. These results are summarized in Table 2. Ions represented in the dissociation scheme for doxorubicin (Fig. 3) are bolded in the table. This data yields supplementary information on the fragmentation pathways of doxorubicin. For example, the MS^3 data shows that *m/z* 333 can be formed by *m/z* 361, a fragment involving the side chain of doxorubicin and epirubicin.

Accurate mass data were collected on an electrospray-time of flight (ESI-TOF) instrument, with internal calibration using a dual-spray source with a continuous flow of calibration mix. Very good accuracies (low ppm) were obtained for most product ions. This instrument did not allow precursor ion selection, therefore fragment ions were formed by increasing the voltage at the end of the capillary in the source (fragmentor voltage) [35]. These results are listed in Table 3, along with corresponding resolutions and relative intensities of the ions. The information gained from these experiments aided the elucidation of the fragmentation scheme and the ion structures for all major ions formed from protonated doxorubicin (see Fig. 3).

A fragmentation scheme (Fig. 3) has been proposed using data generated from collision-induced dissociation experiments and accurate mass measurements. In the cases where the protonation site is not specified in the structures shown in the scheme, the *m/z* values have a (H^+) symbol next to them to remind the reader that the structure shown is not an ion unless it is protonated. It has been previously reported [21] that the initial site of protonation of anthracycline antibiotics occurs on the oxygen of the glycosidic bond, mainly due to the prominent fragmentation with bond breakage at that position, with the oxygen atom remaining on either the aglycone portion (e.g., *m/z* 415, 130) or the sugar moiety (e.g., *m/z* 397, 148). In both cases, the proton can remain attached to the aglycone or the sugar. For the ion at *m/z* 361, the charge is shown localized on the side chain, in order to rationalize its formation from *m/z* 379 (with protonation at the side chain). Proposed ion structures are given for all the major ions produced after activation of the protonated doxorubicin molecule. The initial water loss (*m/z* 526) is proposed to occur from the hydroxyl function attached directly to the A

Table 3
Accurate mass data for doxorubicin product ions

m/z (measured)	*m/z* (calculated)	Formula	Mass accuracy (ppm)	% Intensity	Resolution
86.0612	86.0600	$C_4H_8NO^+$	13.5	[a]	3406
113.0609	113.0597	$C_6H_9O_2^+$	10.6	[a]	3723
130.0861	130.0863	$C_6H_{12}NO_2^+$	−1.2	8	4360
148.0969	148.0968	$C_6H_{14}NO_3^+$	0.5	[a]	4433
306.0545	306.0523	$C_{18}H_{10}O_5^{\bullet+}$	7.3	7	5958
321.0761	321.0758	$C_{19}H_{13}O_5^+$	1.1	100	6158
333.0759	333.0758	$C_{20}H_{13}O_5^+$	0.5	15	6754
346.0464	346.0472	$C_{20}H_{10}O_6^{\bullet+}$	−2.3	7	6191
361.0708	361.0707	$C_{21}H_{13}O_6^+$	0.4	51	6528
379.0820	379.0812	$C_{21}H_{15}O_7^+$	2.0	50	6712
397.0917	397.0918	$C_{21}H_{17}O_8^+$	−0.2	56	7005
415.1040	415.1024	$C_{21}H_{19}O_9^+$	4.0	[a]	6959
526.1700	526.1708	$C_{27}H_{28}NO_{10}^+$	−1.5	2	8070
544.1806	544.1813	$C_{27}H_{30}NO_{11}^+$	−1.4	17	7669

[a] Ions measured from loop injections of doxorubicin (see Section 2).

ring. A second water loss, most probably occurs from the side chain on the A ring. Alternatively, the structure of *m/z* 508 from doxorubicin could potentially be derived from a water molecule being lost from the sugar moiety. The cleavage of the aglycone portion from the sugar can occur on either side of the oxygen of the glycosidic bond. Therefore, we get *m/z* 415 or 397 for the charged aglycone portion or *m/z* 148 and 130 for the protonated sugar. Further fragmentation of the aglycone ion consists of neutral losses of water (*m/z* 415 → 397 → 379 → 361), CO (*m/z* 361 → 333) or the side chain on the A ring (*m/z* 379 → 321).

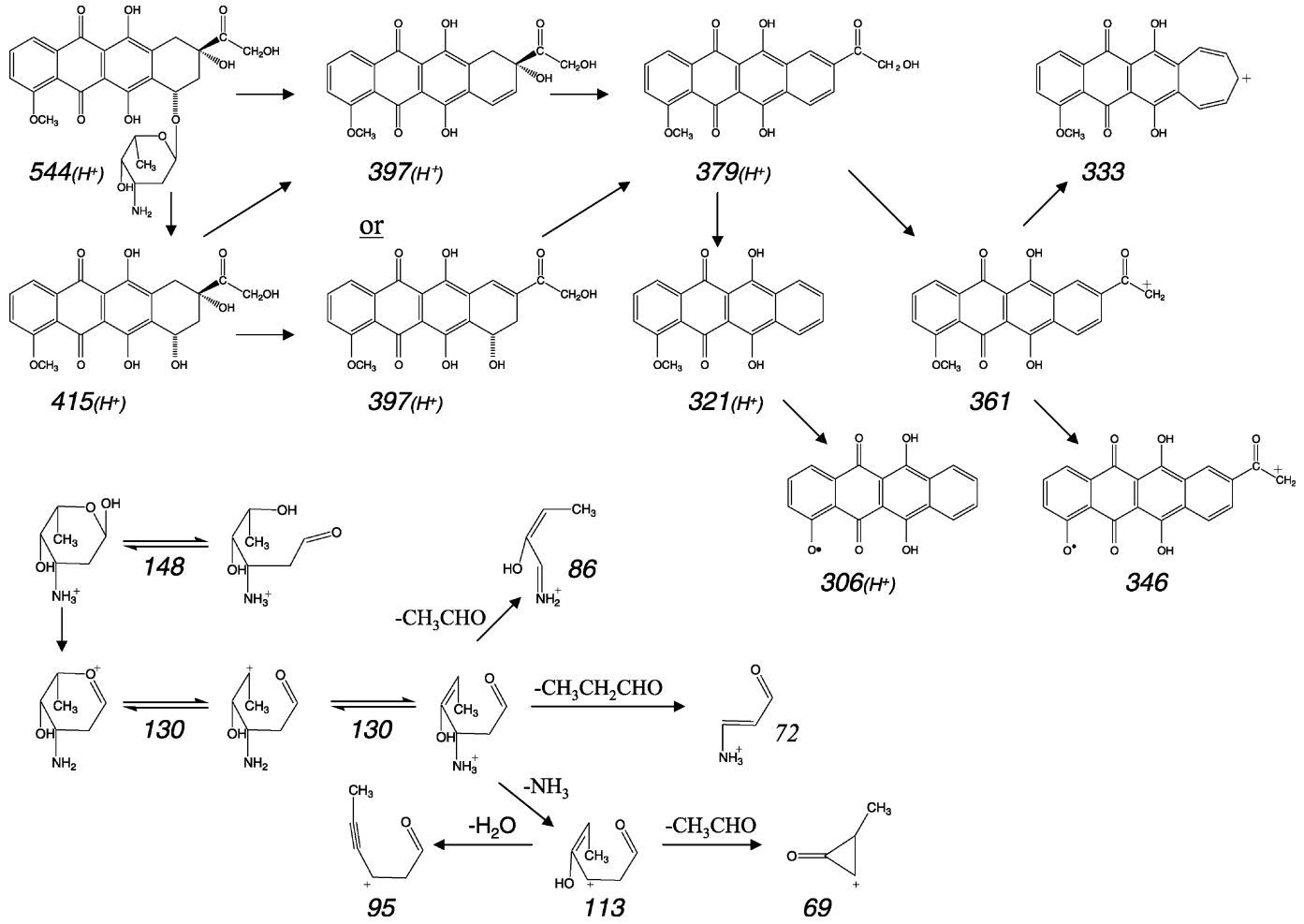

Fig. 3. Proposed fragmentation scheme for doxorubicin. Note that a proton is added next to the mass of the ion for any structure where the protonation site is not specified.

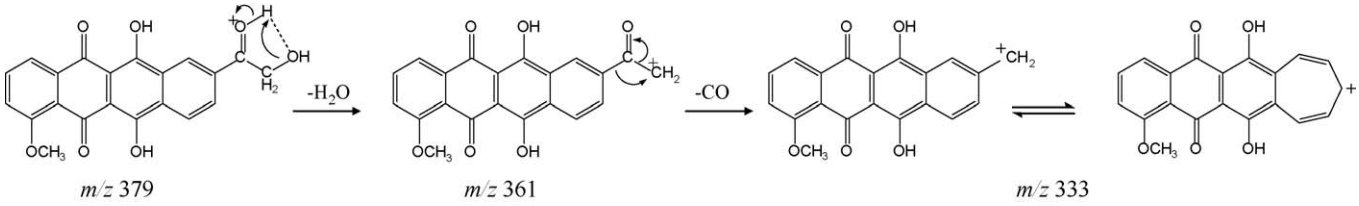

Fig. 4. Proposed fragmentation scheme for the formation of ions at *m/z* 361 and 333 of doxorubicin.

Also, a stable radical ion is formed by the loss of a methyl radical from the methoxy group on the D ring (*m/z* 361 → 346, *m/z* 321 → 306). The product ions at *m/z* 361, 346 and 333 are due to the presence of the hydroxyl group at R_1 (refer to Fig. 1). A water molecule is lost from the side chain of the aglycone ion at *m/z* 379, and the resulting structure is shown in Fig. 3, stabilized by the neighboring carbonyl group (*m/z* 361). This ion can further dissociate by loss of CO to form a stable tropylium-type ion at *m/z* 333. The detailed mechanism proposed for the formation of these two ions is illustrated in Fig. 4.

In the case of the glycosidic bond cleavage occurring with retention of the charge on the sugar portion, *m/z* 148 and 130 (oxonium ion) are formed by bond cleavage on either side of the glycosidic oxygen atom. These two ions are also related by a simple water loss reaction as well. Several fragmentation reactions are rationalized using the linear form of the sugar, which is in equilibrium with the cyclic form (Fig. 3). Ammonia loss from *m/z* 130 yields an ion at *m/z* 113, which can subsequently lose a water molecule forming *m/z* 95. Additionally, the MS^3 results showed a product ion of *m/z* 95 at *m/z* 67, which is likely the product of a facile CO loss from the *m/z* 95 structure shown in Fig. 3. The ion at *m/z* 130 can also further dissociate into *m/z* 86 (loss of CH_3CHO, acetaldehyde) and *m/z* 72 (loss of CH_3CH_2CHO) as seen in the fragmentation scheme. The ion at *m/z* 69 is formed via a similar acetaldehyde loss from *m/z* 113.

All of the pathways discussed above were monitored for the four investigated anthracycline antibiotics under conditions of varying collision energy in the collision cell of a triple quadrupole in order to see if certain pathways are preferred for the different structural analogs.

3.2. Comparing MS/MS behavior of doxorubicin analogs

Fig. 5 represents breakdown curves of the four investigated drugs for the important fragmentation pathways discussed above. The curves are divided into ions of the aglycone portion (with water loss from the protonated molecule as well, on the left of the figure) and ions of the amino sugar (on the right). Each set of curves also has the ion intensity for the precursor ion in order to clarify the importance of each pathway. The most obvious difference, of course, is observed when the side chain is altered, as for daunorubicin and idarubicin, and consequently, several dissociation reactions are absent. This causes the ions at *m/z* 321 and 291 to be more significant for daunorubicin and idarubicin, respectively. Daunorubicin can further dissociate by loss of a methyl radical producing *m/z* 306. Since idarubicin does not have the possibility for any neutral loss occurring due to the side chain of the A ring, nor is it able to lose the methyl radical from the D ring, it seems to exhibit no further fragmentation in comparison to the other three molecules at higher collision energies. There is, however, another pathway occurring above collision energies of 60 V with two main product ions at *m/z* 217 and 189. The structures of these ions can be easily rationalized from *m/z* 291. Fig. 6 illustrates the appearance curves for these ions as well as our proposed mechanism for their formation. The keto functional group is the most likely position for the proton, which is initially removed by the OH group adjacent for a facile loss of H_2O. Then a double CO loss forms *m/z* 217, which can then cleave a further CO group for the final structure shown for *m/z* 189. These types of dissociations were not seen for the other anthracyclines under the energy regime monitored, since they had other reactions possible.

In Fig. 5, epirubicin is shown to have a much larger relative abundance of the ion resulting from a single water loss from its protonated molecule as compared to doxorubicin. This is assumed to be due to the different position of the hydroxyl group in the sugar, causing a more favorable orientation for water to be lost from that part of the molecule (syn elimination of the OH and H groups). Also, idarubicin seems to have a much larger contribution due to the charge being retained on the sugar compared to the other anthracyclines. This is presumably due to the decrease in stability of the aglycone portion as a protonated product in comparison to the daunosamine sugar. The methoxy group could therefore be very important in the overall stability of the aglycone ion (vide infra).

3.3. Computational calculations of ion stabilities

Computational data also aided in the mass spectral characterization of these small molecules. Absolute proton affinity (APA) values were calculated, with the proton residing on each atom with a lone pair of electrons, for daunosamine and 4′epi daunosamine ions (*m/z* 148). Not surprisingly, the charged amino function proved to be the structure with the highest proton affinity in the case of both sugars. The APA values were 223.7 and 222.2 kcal/mol for daunosamine and 4′epi daunosamine, respectively. However, these sugars can easily revert to their linear forms, therefore the discussion of APA becomes less relevant, since the calculations were performed for the cyclic structures. The fragmentation scheme proposed in Fig. 3 rationalizes several sugar-derived product ions from the linear form of the original sugar ions at either *m/z* 148 or 130.

Idarubicin exhibits a much more prevalent ion current for fragment ions retaining the charge on the sugar portion compared

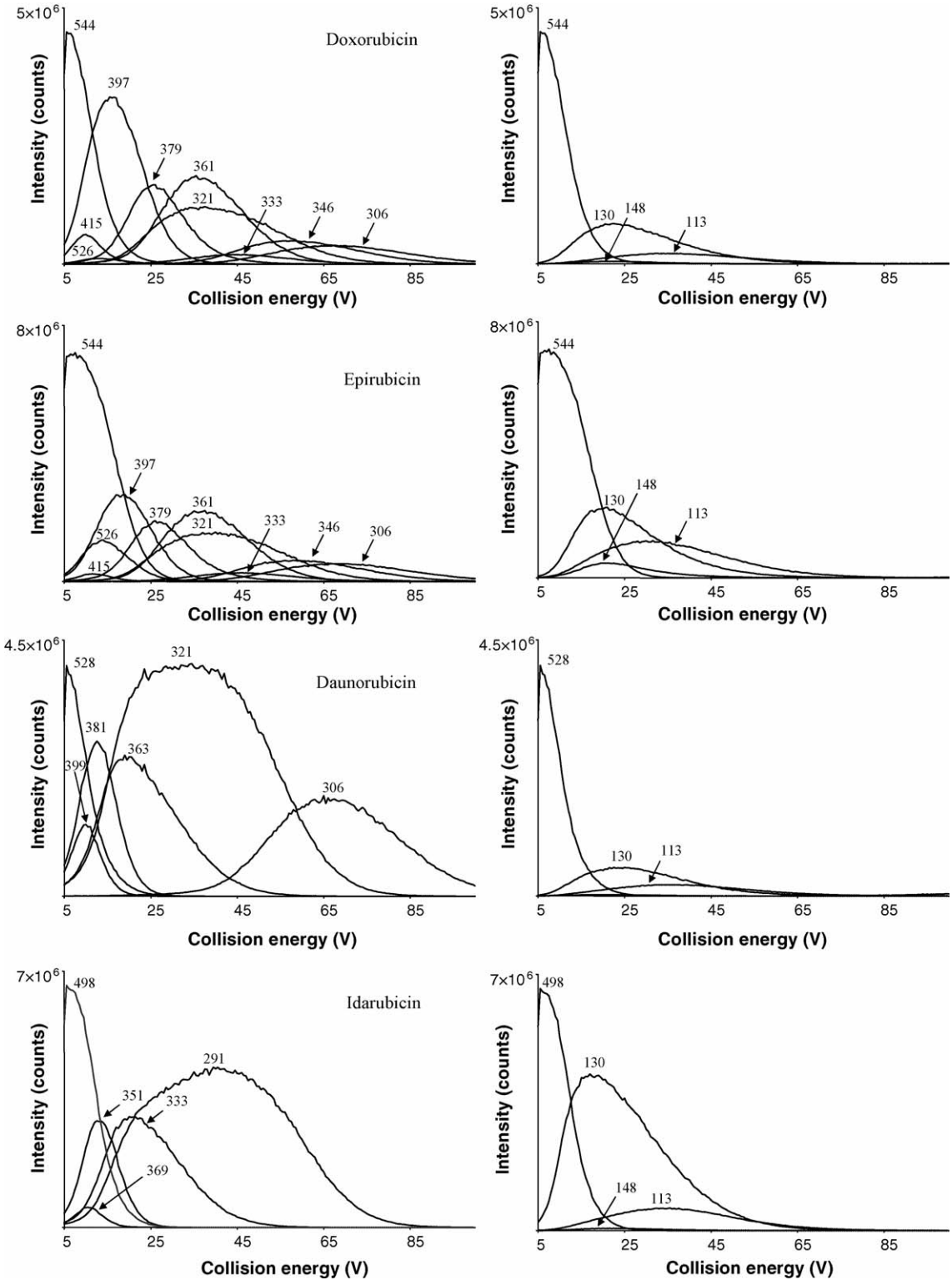

Fig. 5. Breakdown curves showing differences between pathways of analogs.

to the other three investigated compounds. This would indicate a lower stability of its protonated aglycone portion for this ion. The sole difference between the structures of daunorubicin and idarubicin is the presence of the methoxy group at R_2 (see Fig. 1). It was thought that this group is important for the stabilization of the charge on the aglycone portion of the molecule. This theory was tested through the localization of the proton on the different possible sites for daunorubicin. The absolute proton affinities for different protonation sites of the aglycone portion of daunorubicin (*m*/*z* 381) were calculated and are shown in Fig. 7. It is important to note that each oxygen group was tested in these calculations as the location of the proton. However, certain

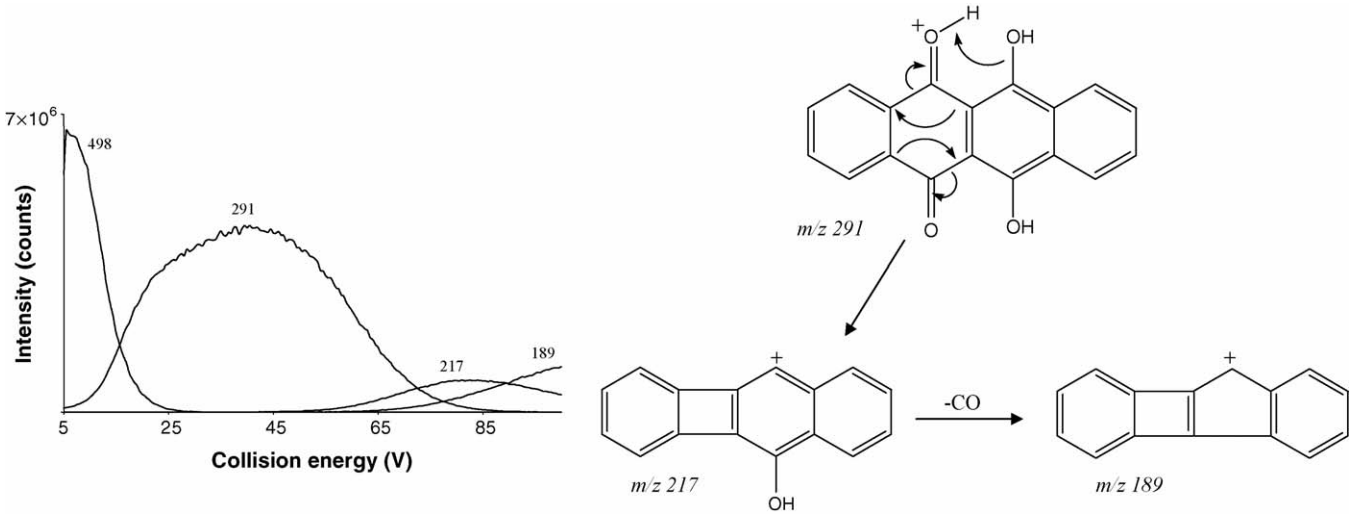

Fig. 6. Specific dissociation reactions for idarubicin under investigated energy regime.

groups, namely the hydroxyl and methoxy groups, did not retain the proton after geometry optimization, and instead reverted to the closest carbonyl oxygen. Also, the carbonyl group next to the methoxy group was evaluated with the proton stabilized either by the methoxy or hydroxy groups on either side. The highest proton affinity is seen for the carbonyl on the bottom of the C ring with the proton pointing in the direction of the methoxy group (222.1 kcal/mol). This further exemplifies the importance of the methoxy group in the proton affinity of the aglycone protonated moiety.

Computational studies were also performed to characterize possible ion structures shown for *m*/*z* 333 (formed via *m*/*z* 361) in the fragmentation scheme (Fig. 3). Two structures were modeled, either with the side chain portion (CH_2^+) residing outside of the ring as well as being incorporated in the aromatic system through ring expansion into the seven-membered ring system,

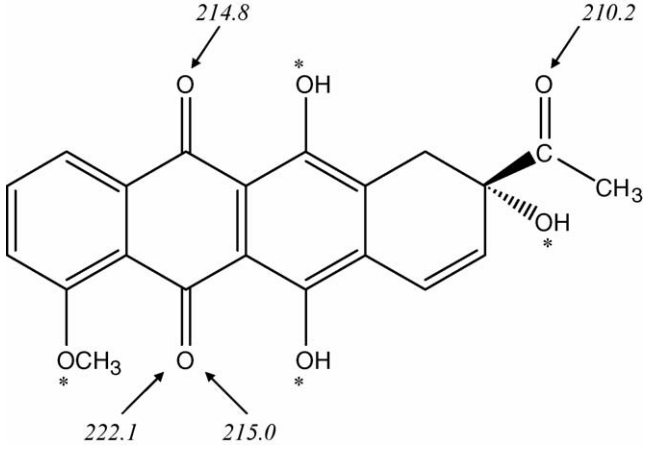

Fig. 7. Absolute proton affinities (in kcal/mol) for different protonation sites of the aglycone portion of daunorubicin (at *m*/*z* 381). Note that for groups designated with (*), the proton did not remain localized here after geometry optimization and reverted to the closest carbonyl O in each case. The values shown on the bottom carbonyl group correspond to the $-\Delta H$ of protonation for the ion structures with the proton pointing in the direction of the methoxy (left) or hydroxy (right) groups, where the actual APA is the highest of the two values.

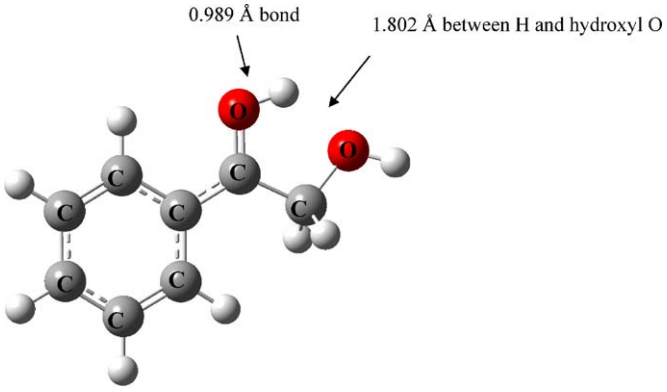

Fig. 8. Computational results for a simplified model system, showing the contribution of the hydroxy group in stabilizing the proton on the carbonyl oxygen of the side chain. Hydrogen bonding is shown between the hydroxy oxygen and the proton on the carbonyl. This geometry (optimized at the B3LYP/6-311+G** level) helps rationalize the pathway for the side chain water loss (seen in Fig. 4).

forming a tropylium-type ion. The latter ion was demonstrated to be of lower energy than the benzyl cation by 8.5 kcal/mol.

In the proposed fragmentation scheme for doxorubicin (Fig. 3), the water loss from *m*/*z* 379 was rationalized as involving the proton residing on the carbonyl of the side chain. A model system (benzene ring with R_1 side chain) was used to confirm the contribution of the hydroxyl group on the side chain in the stabilization of the protonated carbonyl O (Fig. 8). A hydrogen bond is present in this structure between the proton and the oxygen from the hydroxyl group (1.802 Å). These results coincide well with the fragmentation shown in Fig. 4.

In general, these calculations allowed possible ion structures and pathways to be confirmed from the proposed fragmentation schemes of doxorubicin and its analogs as well as help explain the differences in the dissociation behavior of these molecules.

4. Conclusions

Doxorubicin and three of its structural analogs also used in cancer therapy, epirubicin, daunorubicin and idarubicin, were

studied by tandem mass spectrometry with electrospray ionization. MS/MS analysis led to several structurally informative fragments, and differences between the fragments were seen due to small alterations to the functional groups in these molecules. Doxorubicin was considered for the detailed study of the dissociation reactions by collision-induced dissociation (CID), MS^3 experiments and accurate mass measurements. Subsequently, the important fragments for each of the four molecules were monitored at increasing collision energies in order to visualize the differences in stabilities of the product ions. With the aid of computational data, further evidence was shown for the mechanisms presented here. This approach proved very useful for the understanding of fragmentation mechanisms in general and studying the varying stabilities of ion structures in the gas-phase following ion activation under low energy CID conditions. Also, the use of computational data can help support differences in fragmentation mechanisms and resulting product stabilities for similar compounds. Furthermore, a detailed study of the fragmentation of structural analogs can help shed light on the importance of certain functional groups in the stabilities of resulting product ions and can be used to elucidate unknown structures of related compounds, as in the case of metabolism studies and the analysis of degradation products, impurities or synthetic by-products.

Acknowledgements

The authors would like to thank Dr. Julie Marr from Agilent for her help with the accurate mass measurements on the ESI-TOF instrument. Funding is acknowledged from NSERC, the Killam Trust, the National Research Council's Graduate Student Scholarship Supplement Program and the Sumner Foundation.

References

[1] T.W. Sweatman, M. Israel, in: B.A. Teicher (Ed.), Cancer Therapeutics: Experimental and Clinical Agents, Humana Press, Totowa, NJ, 1997, p. 113.
[2] F. Arcamone, Doxorubicin Anticancer Antibiotics, Medicinal Chemistry: A Series of Monographs, vol. 17, Academic Press, London, 1981.
[3] C. Monneret, Eur. J. Med. Chem. 36 (2001) 483.
[4] D.A. Gewirtz, Biochem. Pharmacol. 57 (1999) 727.
[5] A.J. Coukell, D. Faulds, Drugs 53 (1997) 453.
[6] F. Arcamone, L. Bernardi, P. Giardino, B. Patelli, A. Di Marco, A.M. Casazza, G. Pratesi, P. Reggiani, Cancer Treat. Rep. 60 (1976) 829.
[7] F. Lachâtre, P. Marquet, S. Ragot, J.M. Gaulier, P. Cardot, J.L. Dupuy, J. Chromatogr. B 738 (2000) 281.
[8] C. Sottani, G. Tranfo, M. Bettinelli, P. Faranda, M. Spagnoli, C. Minoia, Rapid Commun. Mass Spectrom. 18 (2004) 2426.
[9] R.D. Arnold, J.E. Slack, R.M. Straubinger, J. Chromatogr. B 808 (2004) 141.
[10] D.J. Taatjes, G. Gaudioano, K. Resing, T.H. Koch, J. Med. Chem. 39 (1996) 4135.
[11] R.A. Luce, P.B. Hopkins, Meth. Enzymol. 340 (2001) 396.
[12] S.M. Cutts, A. Nudelman, A. Rephaeli, D.R. Phillips, IUBMB Life 57 (2005) 73.
[13] S. Takanashi, N.R. Bachur, J. Pharmacol. Exp. Ther. 195 (1975) 41.
[14] S. Takanashi, N.R. Bachur, Drug Metab. Dispos. 4 (1976) 79.
[15] G. Cassinelli, E. Confligliacchi, S. Penco, G. Rivola, F. Arcamone, L. Ferrari, Drug Metab. Dispos. 12 (1984) 506.
[16] L. Quintieri, C. Geroni, M. Fantin, R. Battaglia, A. Rosato, W. Speed, P. Zanovello, M. Floreani, Clin. Cancer Res. 11 (2005) 1608.
[17] N.R. Bachur, J. Pharmacol. Exp. Ther. 177 (1971) 573.
[18] K.E. Chan, E. Watson, J. Pharm. Sci. 67 (1978) 1748.
[19] J. Bloom, P. Lehman, M. Israel, O. Rosario, W. Korfmacher, J. Anal. Tox. 16 (1992) 223.
[20] R.G. Smith, Anal. Chem. 54 (1982) 2006.
[21] C. Monneret, N. Sellier, Biomed. Environ. Mass Spectrom. 13 (1986) 319.
[22] K.H. Maurer, U. Rapp, in: A. Frigerio, N. Castagnoli (Eds.), Advances in Mass Spectrometry in Biochemistry and Medicine, Vol. I, Spectrum Publications, New York, 1976, p. 541.
[23] B. Gioia, E. Arlandini, A. Vigevani, Biomed. Mass Spectrom. 11 (1984) 35.
[24] C. Dass, R. Sehadri, M. Israel, D.M. Desiderio, Biomed. Environ. Mass Spectrom. 17 (1988) 37.
[25] C.J. Chandler, R.T. Brownlee, R.J. Hook, D.R. Phillips, J.A. Reiss, J.A. Edgar, Biomed. Environ. Mass Spectrom. 17 (1988) 21.
[26] M.J. Frisch, G.W. Trucks, H.B. Schlegel, G.E. Scuseria, M.A. Robb, J.R. Cheeseman, J.A. Montgomery Jr., T. Vreven, K.N. Kudin, J.C. Burant, J.M. Millam, S.S. Iyengar, J. Tomasi, V. Barone, B. Mennucci, M. Cossi, G. Scalmani, N. Rega, G.A. Petersson, H. Nakatsuji, M. Hada, M. Ehara, K. Toyota, R. Fukuda, J. Hasegawa, M. Ishida, T. Nakajima, Y. Honda, O. Kitao, H. Nakai, M. Klene, X. Li, J.E. Knox, H.P. Hratchian, J.B. Cross, V. Bakken, C. Adamo, J. Jaramillo, R. Gomperts, R.E. Stratmann, O. Yazyev, A.J. Austin, R. Cammi, C. Pomelli, J.W. Ochterski, P.Y. Ayala, K. Morokuma, G.A. Voth, P. Salvador, J.J. Dannenberg, V.G. Zakrzewski, S. Dapprich, A.D. Daniels, M.C. Strain, O. Farkas, D.K. Malick, A.D. Rabuck, K. Raghavachari, J.B. Foresman, J.V. Ortiz, Q. Cui, A.G. Baboul, S. Clifford, J. Cioslowski, B.B. Stefanov, G. Liu, A. Liashenko, P. Piskorz, I. Komaromi, R.L. Martin, D.J. Fox, T. Keith, M.A. Al-Laham, C.Y. Peng, A. Nanayakkara, M. Challacombe, P.M.W. Gill, B. Johnson, W. Chen, M.W. Wong, C. Gonzalez, J.A. Pople, Gaussian 03, Revision B. 05, Gaussian Inc, Wallingford, CT, 2004.
[27] A.D. Becke, J. Chem. Phys. 98 (1993) 5648.
[28] C. Lee, W. Yang, R.G. Parr, Phys. Rev. B 37 (1988) 785.
[29] A.P. Scott, L. Radom, J. Phys. Chem. 100 (1996) 16502.
[30] L. Sleno, D.A. Volmer, B. Kovačević, Z.B. Maksić, J. Am. Soc. Mass Spectrom. 15 (2004) 462.
[31] R. Hilal, S.A.K. Elroby, Int. J. Quantum Chem. 103 (2005) 449.
[32] S.F. Boys, F. Bernardi, Mol. Phys. 19 (1970) 553.
[33] Z. Tozuka, H. Kaneko, T. Shiraga, Y. Mitani, M. Beppu, S. Terashita, A. Kawamura, A. Kagayama, J. Mass Spectrom. 38 (2003) 793.
[34] G. Hopfgartner, E. Varesio, V. Tschäppät, C. Grivet, E. Bourgogne, L.A. Leuthold, J. Mass Spectrom. 39 (2004) 845.
[35] W. Weinmann, M. Stoertzel, S. Vogt, J. Wendt, J. Chromatogr. A 926 (2001) 199.